Uniform NH_4TiOF_3 mesocrystals prepared by an ambient temperature self-assembly process and their topotaxial conversion to anatase†

Lei Zhou, David Smyth Boyle and Paul O'Brien*

Received (in Cambridge, UK) 8th August 2006, Accepted 27th September 2006
First published as an Advance Article on the web 17th October 2006
DOI: 10.1039/b611476h

For the first time, we describe a simple, room-temperature surfactant-mediated route to inorganic mesocrystals of NH_4TiOF_3 and their remarkable topotaxial conversion by washing or annealing to TiO_2 as anatase mesocrystals.

There is considerable interest in the preparation of inorganic mesostructured materials as mesocrystals. In contrast to widely reported conventional mesoporous materials, which place emphasis on a regular pore structure and possess amorphous or polycrystalline channel walls, mesocrystals are quasi-single crystals comprising ordered assemblies of small vectorially aligned nanocrystallites to form an entirely new class of porous material superstructures.[1] Mesocrystals and their syntheses also provide a challenge to accepted views on crystal growth,[2] as most are typically described by a process of nucleation and growth and/or Ostwald ripening. Moreover, by using low temperature soft-chemical routes, these systems may also offer a paradigm to mimic assembly processes that govern the formation of bioinorganic materials.[3] Such composite crystals are of considerable interest to a broad range of disciplines including the chemical and life sciences.

The inorganic semiconductor titanium dioxide has been extensively studied because it has a wide range of applications, including in: photocatalysis,[4–7] amphiphilic coating,[8] and dye-sensitized solar cells.[9,10] A variety of nanostructured morphologies have been reported including spheres,[11–13] porous films,[14,15] nanofibers,[16] nanowires[17] and nanotubes.[18] However, the formation of TiO_2 mesocrystals and crystalline, non-silica mesoporous oxides in general remains a challenge.[19,20] In this Communication, we describe the formation of uniform mesocrystals of NH_4TiOF_3 comprising orientationally ordered primary crystallites, and their remarkable topotaxial conversion to an architecturally analogous mesocrystal of TiO_2 as anatase.

Precipitates collected from the reaction mixture after different reaction times (see Notes and references for experimental details‡) indicate that the particles grow over a 16 h period to their final sizes. Particles isolated from the reaction after 20 h are remarkably regular in shape and size, as evidenced by scanning electron microscopy (Fig. 1a). The mean edge length and thickness of as-prepared particles (Fig. 1b, d, f) are 3.45 ± 0.25 μm and 0.78 ± 0.09 μm respectively. The difference between shorter and longer edge lengths of the almost square particles is less than 5%. Most of the particles have edge lengths between 3.2 μm and 3.8 μm. It is clear from powder X-ray diffraction (p-XRD) and FT-IR (see ESI† Table A and Fig. A) that the dominant phase in the

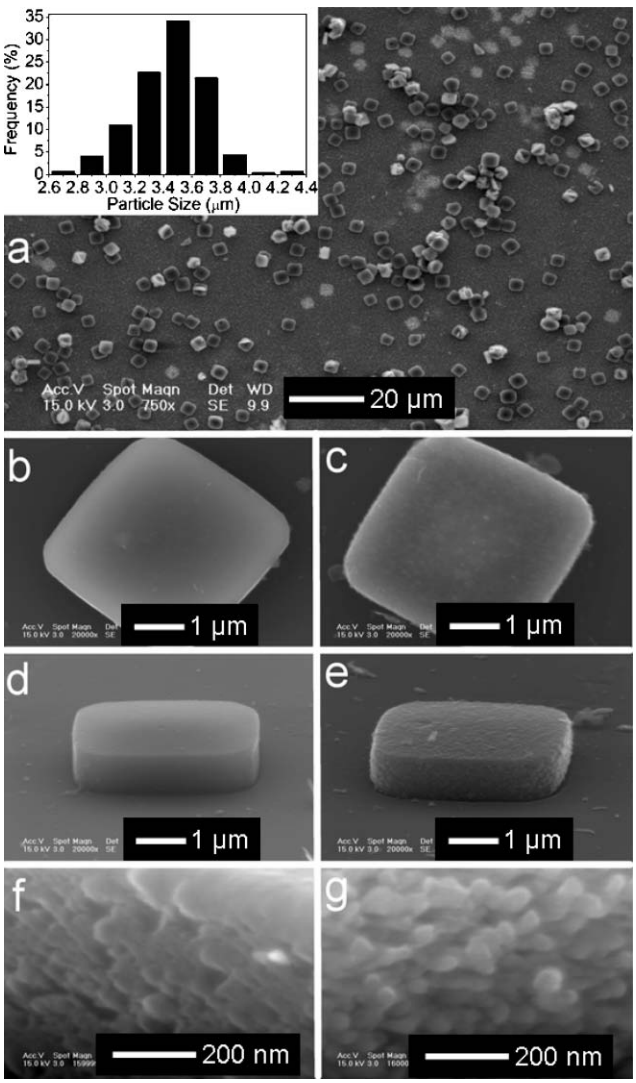

Fig. 1 SEM images of the particles precipitated in the presence of 23.1 wt% Brij 58 at 35 °C for 20 h and the particles sintered at 450 °C for 2 h. (a) An overall view of the as-prepared particles. Inset is the size distribution for these particles. (b–c) Top views of an as-prepared particle and a sintered particle. (d–e) Cross-sectional views of an as-prepared particle and sintered particle. (f–g) High-magnification cross-sectional images of an as-prepared and sintered particle respectively.

School of Chemistry and Manchester Materials Science Centre, University of Manchester, Oxford Road, Manchester, UK M13 9PL. E-mail: paul.obrien@manchester.ac.uk; Fax: (+)44 (0)161 275 4658; Tel: (+)44 (0)161 275 4653

† Electronic supplementary information (ESI) available: Powder XRD (p-XRD), FT-IR and thermogravimetric analysis (TGA) of as-prepared and processed NH_4TiOF_3 particles. Video data demonstrating identical electron diffraction from different regions of NH_4TiOF_3 and TiO_2 mesocrystals. See DOI: 10.1039/b611476h

as-prepared particles is NH_4TiOF_3.[21] No signals deriving from the surfactant (Brij 58) are observed. Moreover, after sintering in air at 450 °C for 2 h, the mean edge length and thickness (Fig. 1c, e, g) remained the same (3.49 ± 0.27 μm and 0.80 ± 0.10 μm). The effect of sintering on the morphology is shown in Fig. 1b–g. The shape and size of the particles are not altered upon sintering, but the surface roughness increases.

The conversion of NH_4TiOF_3 to TiO_2 with retention of orientation has been proposed[22] but not reported previously. Remarkably, results obtained during these studies indicate that after washing with aqueous H_2BO_3, the NH_4TiOF_3 phase is transformed to the anatase form of TiO_2 as an analogous mesocrystal. Identical results were obtained through sintering in air. The nature of these particles, after washing with dilute boric acid (H_2BO_3, 35 °C for 2 h) or sintering in air (450 °C for 2 h), was investigated by p-XRD (see ESI† Fig. B). According to the results of elemental analysis of as-prepared NH_4TiOF_3 particles, the C content is below <0.3%, which suggests little incorporation of surfactant (*e.g.* Brij 58) in the as-prepared samples, in agreement with FT-IR data. The Ti and N content are 33.56% and 9.44% respectively; the Ti/N ratio is 0.28, close to the predicated value of 0.29 for pure NH_4TiOF_3. Hence it is a reasonable assumption that NH_4TiOF_3 is the only source of Ti and N. Thermogravimetric analysis (TGA) of as-prepared material (see ESI† Fig. C) indicates there is about 47% mass loss through heating to 450 °C (*cf.* predicated value of 40% for the conversion of as-prepared NH_4TiOF_3 to TiO_2, the discrepancy ascribed to chemisorbed water and trace impurities within pores of the as-synthesised mesocrystal) and above 450 °C no mass loss was detected. Further analysis suggests the existence of unstable intermediate phases (*e.g.* $HTiOF_3$ and $TiOF_2$) during the heating process.

The Scherrer equation was used to determine mean crystallite dimensions, calculated to be ~26 nm in the [100]/[010] directions and ~38 nm in the [001] direction before sintering, and ~24 nm in the [100]/[010] directions and ~16 nm in the [001] direction after sintering. The shrinkage in the [100]/[010] directions during thermal transformation is about 8%, which is to be expected on the basis that there is little change in the relevant lattice parameters for the compounds. In the [001] direction, the shrinkage is about 58%, consistent with a theoretical value of 63% calculated from the cell parameters. The pattern of results is confirmed through the high-magnification SEM images shown in Fig. 1f and 1g. Before sintering, the samples appear as tightly packed aggregates of small particles with sizes in the range approximately 30–60 nm. After sintering, particle dimensions reduce to approximately 15–35 nm, with a corresponding increase in the dimensions of voids in the mesocrystal which consequently become more readily observable.

Transmission electron microscopy (TEM) provides more details of the structure of the as-prepared NH_4TiOF_3 mesocrystals (Fig. 2). The regions of low contrast between individual crystallites indicate interstices with diameters of about 5–10 nm exist within these particles (Fig. 2b). The interstitial walls are formed by nanocrystals whose lengths can extend to 25 nm or more, which is consistent with the 26 nm in the [100]/[010] directions from the XRD results. Selected area electron diffraction (SAED) of an area ~250 nm in diameter (Fig. 2a) shows single-crystal diffraction with minor distortions, indicating that the whole assembly of particles behaves as a single crystal. The distortions come from the mismatch between boundaries of the small particles, which are

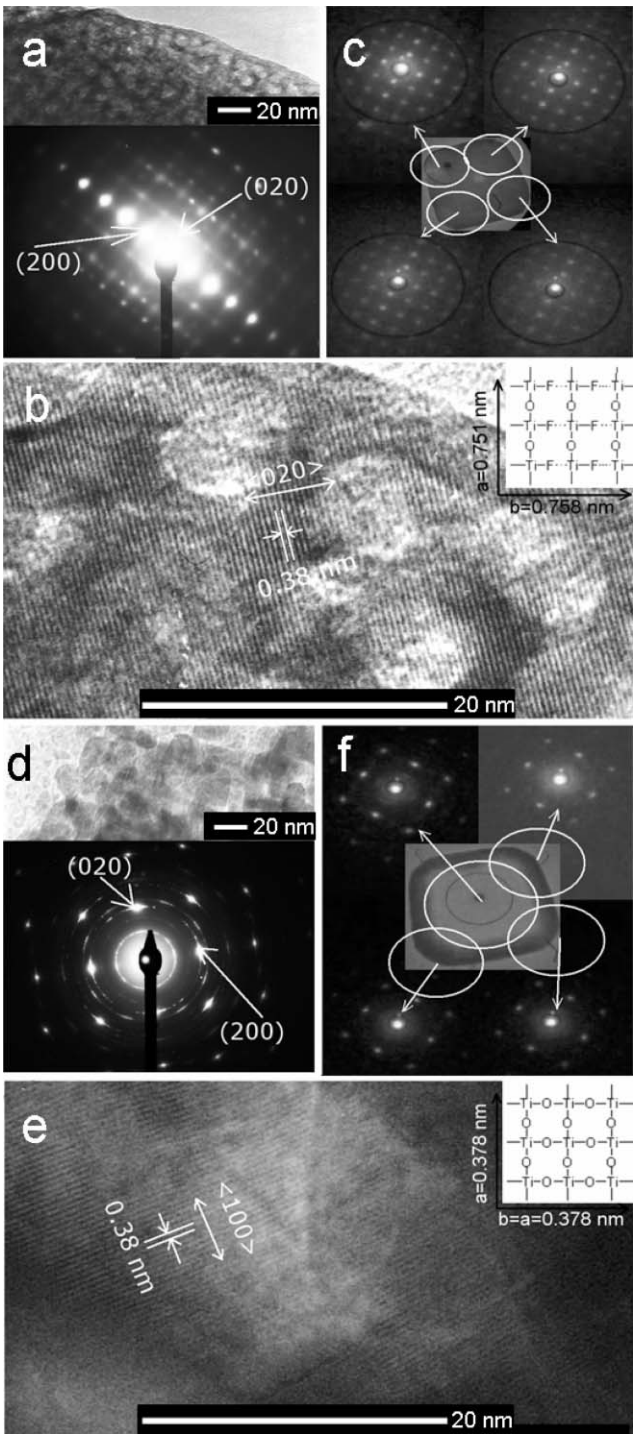

Fig. 2 TEM images and SAED patterns of samples precipitated in the presence of 23.1% Brij 58 at 35 °C for 20 h and those after sintering at 450 °C for 2 h. (a) Low-magnification TEM image of the sample before sintering and corresponding SAED pattern. (b) High-magnification TEM image of the sample before sintering. (c) Images taken from a video recorded during the process of moving a hollowed sample in TEM in diffraction mode. (d) Low magnification TEM image of the sintered sample and corresponding SAED pattern. (e) High resolution TEM image of the sintered sample. (f) Still images taken from the video, which shows identical diffraction from different parts of a hollowed sample.

typical for a mesocrystal.[1] Importantly, when the sample was moved in the microscope in diffraction mode, the pattern remained the same, except for some minor brightness changes (see ESI† Video 1). In Fig. 2c, some video capture images are shown.

TEM images of TiO_2 mesocrystals obtained by topotaxial conversion of NH_4TiOF_3 are shown in Fig. 2d–e. The individual TiO_2 particles comprising the mesocrystal are most apparent. These particles have a critical dimension of about 20 nm, which again is consistent with the XRD result (24 nm in the [100]/[010] directions). The anatase form of TiO_2 ($a = b = 3.7845$ Å, $c = 9.5143$ Å) has a similar crystal structure to NH_4TiOF_3 ($a = 7.5594$ Å, $b = 7.5754$ Å, $c = 12.7548$ Å) in the *ab* planes, which are illustrated as insets within Fig. 2b and e. The lattice mismatch is below 0.12%.

The processes involved in the growth of the initial NH_4TiOF_3 mesocrystals will be described in detail elsewhere; for convenience, these processes can be divided into three stages *viz*. phase separation, matrix-mediated mesophase transformation and self-assembly of mesoscale building blocks. In the first stage, PEO moieties ($-(OCH_2CH_2)_n$) on surfactants interact with metal centres/condensed metal-oxo species in the solution as Lewis base O-donors. Condensation between these moieties leads the surfactants to coalesce, producing a new viscous phase with high surfactant concentration. Support for this interpretation is borne out empirically; a subsequent addition of water yields a clear solution, consistent with formation of highly concentrated surfactant phases (SAED data suggest these microphases are not crystallized). In the second stage, these small particles aggregate through cooperative reorganization of inorganic and organic components at the mesoscale to form larger hybrid particles. During this step, the particles undergo an amorphous-to-crystalline transformation. The surfactant may act as a matrix for oriented crystallization of inorganic species and the layered structure of NH_4TiOF_3 is beneficial to this matrix-mediated nucleation (surfactants can easily attach on the *ab* planes of NH_4TiOF_3). Nucleation of inorganic species causes micelles of surfactants to unfold, forming a highly uniform matrix. In the final stage, face-specific interactions between the building blocks lead to directed self-assembly of oriented nanocrystals and mesocrystal formation.

Topotaxial transformation to TiO_2 grains could occur *via* the *ab* planes of NH_4TiOF_3 mesocrystals. During such phase transformations, NH_4TiOF_3 could serve as a metastable lattice-matched substrate as well a source of all the Ti atoms and a fraction of the O atoms. Due to the restricted dimensions and low surface interfacial energies, small TiO_2 grains could generate and remain in the same orientation as precursor NH_4TiOF_3. Further oriented nucleation of TiO_2 would be promoted *via* these small grains to develop larger grains and thus consume NH_4TiOF_3. In the *c* direction, TiO_2 has greater atom density and shrinkage should occur. This change has been seen in SEM images and confirmed by XRD data. The corresponding SAED pattern of a zone 3 μm in diameter is shown in Fig. 2d and indicates these particles are mesocrystals. As before, no discernable differences other than brightness perturbations were apparent in patterns obtained through crystal manipulation in TEM diffraction mode. Some still images taken from video recordings (see ESI† Video 2) are shown in Fig. 2f.

In this Communication, we have demonstrated a new synthetic route to remarkably regular inorganic mesocrystals of NH_4TiOF_3 and TiO_2, the latter *via* topotaxial conversion of the former to anatase by washing or thermal conversion. Such intricate control of crystal architecture has parallels with biomineralisation processes that rely on spatial localisation, with conditions of low supersaturation and active interfaces. The method is novel and preliminary results indicate it can be extended to other materials such as ZrO_2.

The authors thank ORS and the University of Manchester for funding.

Notes and references

‡ Synthesis: all chemicals were purchased from Aldrich and employed without further purification. In a typical experiment, 15 g (23.1 wt%) of non-ionic polyoxyethylene surfactant (Brij 58, $C_{16}H_{33}(OCH_2CH_2)_{20}OH$) was added to 50 cm^3 of a freshly prepared, stirred, thermostatted (35 °C) solution of $(NH_4)_2TiF_6$ (0.1 mol dm^{-3}) and H_3BO_3 (0.2 mol dm^{-3}). Boric acid acts as a F-scavenger. In the absence of surfactant, polycrystalline TiO_2 is formed, as reported by others.[23] Stirring was stopped after the surfactant was totally dispersed; the solution was then kept at 35 °C for up to 24 h. Precipitates were collected and separated by centrifugation and washed (×3) sequentially with deionized water, ethanol and acetone. Similar results were obtained using 14.9 wt% Brij 56 ($C_{16}H_{33}(OCH_2CH_2)_{10}OH$) or 16.7 wt% Brij 700 ($C_{18}H_{37}(OCH_2CH_2)_{100}OH$). Thermal treatment of samples was conducted using a Carbolite ESF furnace in ambient air. SEM was performed using a Philips XL30 FEG SEM. Samples were carbon coated using an Edwards Sputter Coater (E306A) prior to analysis. Powder X-ray diffraction studies were performed using a Bruker AXS D8 diffractometer and CuKα radiation (40 kV; graphite monochromated) for 2θ values over 5–90° (steps of 0.05°; count time 5 s). Low angle XRD measurements were recorded using a Philips X'Pert MPD (PW 3040). TEM was performed using a Philips CM 200 (200 kV) instrument. A Seiko SSC/S200 instrument was employed for TGA using a heating rate of 5 °C min^{-1}.

1 H. Cölfen and M. Antonietti, *Angew. Chem., Int. Ed.*, 2005, **44**, 5576.
2 L. Motte, A. Courty, A.-T. Ngo, I. Lisiecki and M.-P. Pileni, in *Nanocrystals forming mesoscopic structures*, ed. M.-P. Pileni, Wiley-VCH, Weinheim, 2005, pp. 1–49.
3 H. Cölfen and S. Mann, *Angew. Chem., Int. Ed.*, 2003, **42**, 2350.
4 A. J. Nozik, *Nature*, 1975, **257**, 383.
5 S. U. M. Khan, M. Al-Shahry and J. W. B. Ingler, *Science*, 2002, **297**, 2243.
6 M. Fujihira, Y. Satoh and T. Osa, *Nature*, 1981, **293**, 206.
7 R. Asahi, T. Morikawa, T. Ohwaki, K. Aoki and Y. Taga, *Science*, 2001, **293**, 269.
8 R. Wang, K. Hashimoto, A. Fujishima, M. Chikuni, E. Kojima, A. Kitamura, M. Shimohigoshi and T. Watanabe, Nature, 1997, 388, 431, *Nature*, 1997, **388**, 431.
9 B. O'Regan and M. Grätzel, *Nature*, 1991, **353**, 737.
10 U. Bach, D. Lupo, R. Comte, J. E. Moser, F. Weissortel, J. Salbeck, H. Spreitzer and M. Grätzel, *Nature*, 1998, **395**, 583.
11 X. C. Jiang, T. Herricks and Y. N. Xia, *Adv. Mater.*, 2003, **15**, 1205.
12 Y. L. Li and T. Ishigaki, *Chem. Mater.*, 2001, **13**, 1577.
13 R. A. Caruso, A. Susha and F. Caruso, *Chem. Mater.*, 2001, **13**, 400.
14 P. D. Yang, D. Y. Zhao, D. I. Margolese, B. F. Chmelka and G. D. Stucky, *Nature*, 1998, **396**, 152.
15 J. E. G. J. Wijnhoven and W. L. Vos, *Science*, 1998, **281**, 802.
16 D. Li and Y. N. Xia, *Nano Lett.*, 2003, **3**, 555.
17 R. L. Penn and J. F. Banfield, *Science*, 1998, **281**, 969.
18 J. H. Lee, I. C. Leu, M. C. Hsu, Y. W. Chung and M. H. Hon, *J. Phys. Chem. B*, 2005, **109**, 13056.
19 P. D. Yang, D. Y. Zhao, D. I. Margolese, B. F. Chmelka and G. D. Stucky, *Chem. Mater.*, 1999, **11**, 2813.
20 G. J. A. A. Soler-Illia, C. Sanchez, B. Lebeau and J. Patar, *Chem. Rev.*, 2002, **102**, 4093.
21 N. M. Laptash, I. G. Maslennikova and T. A. Kaidalova, *J. Fluorine Chem.*, 1999, **99**, 133–137.
22 I. Moriguchi, K. Sonada, K. Matsuo, S. Kagawa and Y. Teraoka, *Chem. Commun.*, 2001, 134.
23 S. Deki, Y. Aoi, O. Hiro and A. Kajinami, *Chem. Lett.*, 1996, **6**, 433.

